Preprints (www.preprints.org) | NOT PEER-REVIEWED | Posted: 11 December 2020 doi:10.20944/preprints202012.0289.v1

Type of the Paper (Article)

Profiling ribonucleotide and deoxyribonucleotide pools perturbed by remdesivir in human bronchial epithelial cells

Yan Li [1,‡], Huixia Zhang [1,‡], Wendi Luo [1], Christopher Wai Kei Lam [2], Caiyun Wang [1], Liping Bai [1], Vincent Kam Wai Wong [1], Wei Zhang [1,*] and Zhihong Jiang [1,*]

[1] State Key Laboratory of Quality Research in Chinese Medicines, Macau Institute for Applied Research in Medicine and Health, Macau University of Science and Technology, Taipa, Macau, China; Guangdong-Hong Kong-Macao Joint Laboratory of Respiratory Infectious Disease (Macau University of Science and Technology)

[2] Faculty of Medicine, Macau University of Science and Technology, Taipa, Macau, China; Guangdong-Hong Kong-Macao Joint Laboratory of Respiratory Infectious Disease (Macau University of Science and Technology)

‡ These authors contributed equally to this work.

* Corresponding authors. E-mail addresses: wzhang@must.edu.mo (W. Zhang), Zhjiang@must.edu.mo (Z. Jiang).

Abstract: Remdesivir (RDV) has garnered much hope for its moderate anti-COVID-19 effects, but its limited amelioration of survival in hospitalized patient causes a huge controversy over the applicability of RDV to COVID-19 treatment. Developing strategies to improve its antivirus efficacy is urgently required. As anticipated, RDV exhibits similar behavior with other nucleotide analogs to disrupt the metabolism of natural endogenous ribonucleotides (RNs) and deoxyribonucleotides (dRNs). Alterations in endogenous RNs and dRNs play a critical role in virus replication as well as other key cellular functions. Thus elucidation of the disturbances of RDV on RNs and dRNs could help to understand its exact mechanism of action. Here, the metabolic profiling determined by liquid chromatography–mass spectrometry method showed a general increase in the abundance of nucleotides and a more than 2-fold increase for specific nucleotides. However, the variation of pyrimidine ribonucleotides was relative slight or even contrary, resulting in obvious imbalance between purine and pyrimidine ribonucleotides, which implied the obstacle of RDV to pyrimidine synthesis and could further block the transcription and replication of viral RNA. Additionally, the extreme disequilibrium between cytidine triphosphate (CTP) and cytidine monophosphate might result from the inhibition of CTP synthase and provide a metabolic target for the treatment of COVID-19 infection. Since nucleotides metabolism pathways are vulnerable to nucleotide analogues and are liable to be the regulation targets, it is promising to enhance the efficacy of RDV through co-administration with CTP synthase inhibitors or de novo pyrimidine synthesis inhibitors to exacerbate the imbalance of nucleotide pools.

Keywords: remdesivir, perturbation of nucleotide pools, inhibition of RNA and DNA synthesis, CTP synthase.

1. Introduction

Remdesivir (RDV), an adenine nucleotide analog that inserts into viral RNA chains resulting in their premature termination [1], has shown a broad-spectrum of antiviral activity against severe acute respiratory syndrome coronavirus (SARS–CoV) [2], Nipah virus [3], Middle East respiratory syndrome coronavirus (MERS–CoV) [4, 5], Ebola virus [6-8] and 2019 novel coronavirus (COVID-19) [9-11]. Because of the advantage of RDV in terms of shortening the time to recovery in adults infected

© 2020 by the author(s). Distributed under a Creative Commons CC BY license.

Preprints (www.preprints.org) | NOT PEER-REVIEWED | Posted: 11 December 2020 doi:10.20944/preprints202012.0289.v1

with COVID-19, the US Food and Drug Administration issued an Emergency Use Authorization for use of remdesivir for the treatment of hospitalized patients with COVID-19 [12]. Based on previous studies, RDV exerts its antivirus activity through specifically inhibiting the activity of viral RdRps, which are crucial to virus survival not only through replication but also as engines of genome variability and evolution, without interference with human RNA polymerase [13, 14].

The success of application of metabolic reprogramming to treat cancer [15] and inflammation [16] prompted us to explore the possibility to exploit it in RDV treatment. RDV shares similar characteristics with other nucleotide analogs, both of which undergo intracellular phosphorylation to their triphosphate metabolites [17, 18]. The phosphate prodrug of RDV contributes to bypass the rate-limiting step during translating the parent nucleoside into its monophosphate, and the further esterification and amidation decrease the polarity of phosphorylated nucleoside and increase its permeability [19, 20]. Although evidences showed that the predominant metabolites RDV *in vivo* and *in vitro* were parent nucleoside and RDV-MP, respectively [21, 22], the bioconversion of RDV-MP to RDV-DP and RDV-TP were mediated by the same kinases involved in natural nucleotides synthesis. Due to metabolic competition with natural nucleotides such as AMP, ADP and ATP, RDV inevitably results in perturbation of endogenous RNs, which could restrict the synthesis of viral RNA in turn [23, 24]. However, to date it remains uncertain to what extent the treatment of RDV in cell results in changes of nucleotide levels.

Besides alteration of adenine nucleotides, RDV might change the levels of other nucleotides via affecting the enzymes in nucleotide synthesis and metabolism. Previous studies have proven that guanine analogs, ribavirin and 5-ethynyl-1-beta-D-ribofuranosylimidazole-4-carboxamide (EICAR) depleted the GTP pool through inhibition of inosinate dehydrogenase [25, 26]. Similarly, RDV as an adenine analog was deduced to inhibit the S-adenosylhomocysteine (SAH) hydrolase and adenylate kinase, consequently interfering with the biosynthesis of adenine derivatives [27, 28]. Moreover, Kim et al have reported previously that SARS coronavirus may require more ATP to promote stable helicase translocation necessary for delicate RNA replication [29]. Endogenous RNs and dRNs pools also affect the response of RDV against viral infection because the disturbance of adenine derivatives will affect the function of RdRPs [30]. Furthermore, unbalanced change of dRNs caused by RDV could induce potential side effects because failure to maintain the dNTPs level causing genetic abnormalities or cell death [31]. This has already been proven that adaptive metabolic reprogramming of RNs and dRNs pools could promote chemotherapy at the early stage of treatment [32]. Thus elucidation of the disturbances of RDV treatment on RNs and dRNs pool sizes will not only permit us to understand the exact mechanism of action of RDV, but also enhance the antivirus activity based on the targeted-regulation of RNs and dRNs.

So far, there has been no report on the effects of RDV on RNs and dRNs pool sizes due mainly to the difficulty of quantifying these pool sizes, particularly for the monophosphate and diphosphate nucleotides. Recently, we describe a simpler, selective and highly sensitive HPLC-MS/MS method for quantification of RNs and dRNs pools in cells after trimethylsilyl diazomethane (TMSD) derivatization [33]. In the present study, the effects of RDV incubation over different time-periods on RNs and dRNs pool sizes of BEAS-2B cells have been investigated using well-established HPLC-MS/MS methodology. Moreover, the influence of RDV on cell cycle, RNA and DNA synthesis and protein expression were studied. The results obtained from this study should facilitate understanding the exact mechanism of RDV and assessment of the efficacy and toxicity of RDV for developing the individualized therapy.

2. Results

2.1. RDV decreased the viability of BEAS-2B cell line

At the beginning of this study, we investigated the cytotoxicity of RDV on BEAS-2B cells by using MTT assays. The cells were treated with RDV at various concentrations (0-100 μM) for 24, 48 and 72 h, respectively. As shown in the results, cell number was gradually decreased as the concentration of RDV increased in all the time points of incubation. The viability of cells presented a

Preprints (www.preprints.org) | NOT PEER-REVIEWED | Posted: 11 December 2020 doi:10.20944/preprints202012.0289.v1

dose- and time- dependent reduces (Figure 1 A). The calculated IC_{50} values in 48 and 72 h were 25.3 ± 2.6 and 9.6 ± 0.7 μM, respectively. 10 μM was chose for the following experiments.

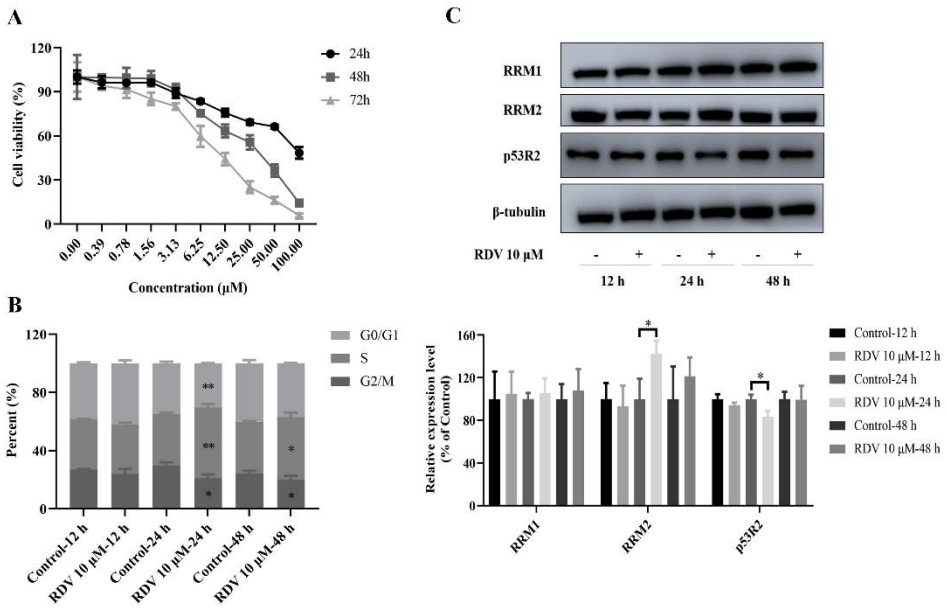

Figure 1. Effects of RDV on (A) cell viability, (B) cell cycle and (C) riboreductase expression in BEAS-2B cells treated with 10 μM RDV. (∗: $P < 0.05$, ∗∗: $P < 0.01$, compared with control group).

2.2. RDV induced S phase arrest in BEAS-2B cells

On account of the significant inhibitory effect on cell viability and proliferation, we investigated the effect of RDV treatment on the distribution of cells in cell cycle under different time point. BEAS-2B cells were treated with or without 10 μM RDV for 12, 24 and 48 h, and subsequently analyzed by flow-cytometry. As shown in Figure 1 B, an altered pattern of cell cycle was observed in BEAS-2B cells exposed to 10 μM RDV and with respect to control. With the incubation time increased, the proportion of cells in S phase significantly increased while the percentage of cells in G2/M phases obviously decreased in comparison to untreated cells. After incubated for 24 h, the percentage of cells in S phase was 35.3 ± 0.75% in control, which gradually increases to 48.69 ± 1.8 % in RDV group ($P < 0.01$). The number of cell in G2 phase decreased from control 29.67 ± 1.59% to 20.81 ± 1.92% of RDV ($P < 0.05$). The resembled results at 48 h was obtained. In brief, RDV can arrest the cells in S phase.

2.3. RDV inhibited RNA and DNA synthesis

In order to detect the effects of RDV on RNA and DNA synthesis in proliferating cells, we performed EU and EdU staining method on the basis of click chemistry. EU and EdU are the structural analogues of uridine and deoxyuridine, respectively. Their triphosphate metabolites compete with UTP and TTP to incorporate into newly synthesized RNA and DNA, respectively, and subsequently reacted with Azide -modified fluorophores. The fluorescence intensity was proportional to the amount of the incorporated EU and EdU in nascent RNA and DNA. As shown in Figure 2 A and B, after incubation with RDV for 14 h, the fluorescence intensity of Alexa594-azide decreased significantly in comparison to control group, indicating the reduction of RNA and DNA synthesis, and the inhibition of proliferation of BEAS-2B cells. Interestingly, not all DAPI stained cells were labeled with EdU. The reason for this phenomenon is that the incorporation of EdU only occurs in S phase during DNA replicating, while DAPI is a nonspecific fluorescent dye with the strong binding ability to the existing or nascent DNA [37].

Preprints (www.preprints.org) | NOT PEER-REVIEWED | Posted: 11 December 2020 doi:10.20944/preprints202012.0289.v1

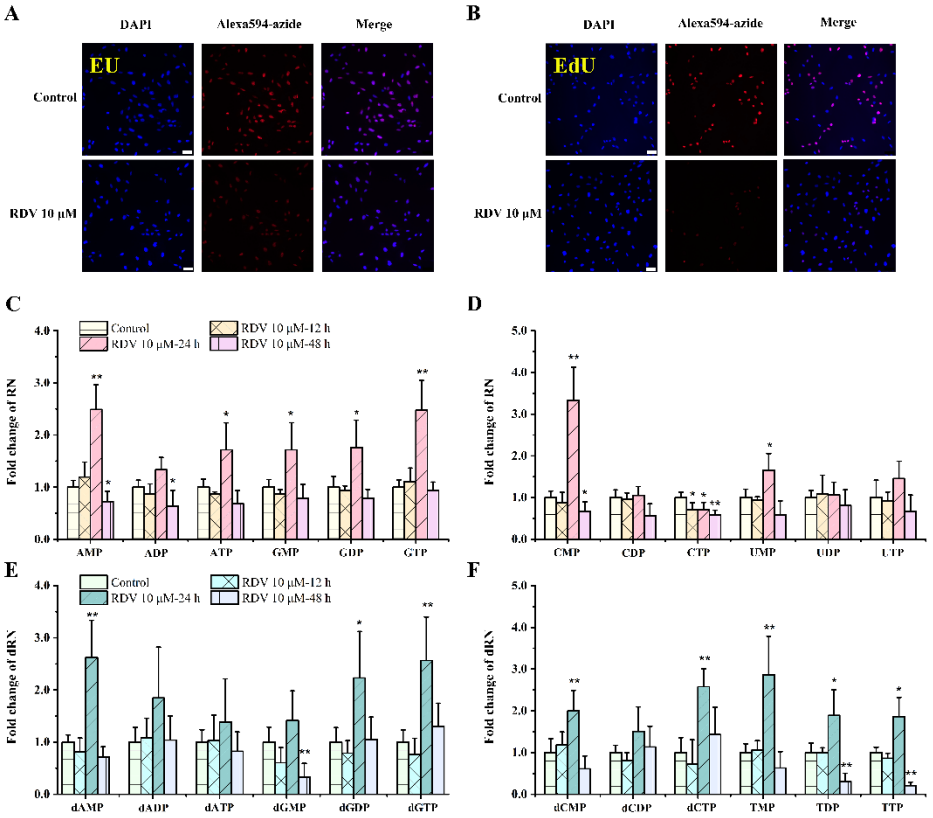

Figure 2. Effects of RDV on the RNA and DNA synthesis (A-B), and on the nucleotide pools (C-F). Fluorescence microscope images (Scale Bars = 100 μm) of EU or EdU-mediated click chemistry indicated that RDV treatment for 14 h inhibited the synthesis of (A) RNA and (B) DNA. Fold changes in nucleotide abundances, as measured by LC/MS-MS, in 10 μM RDV-treated or vehicle-treated BEAS-2B cells for 12, 24 and 48 hours (C-F). (∗: $P < 0.05$, ∗∗: $P < 0.01$, compared with control group).

2.4. Perturbation of RNs and dRNs pool size by RDV in BEAS-2B cells

To examine metabolic reprogramming events that influence the cellular response to virus, we used targeted LC/MS-MS via selected reaction monitoring (SRM) to examine changes in the steady-state metabolomics profile of BEAS-2B cells after exposure to 10 μM RDV with 12 h, 24 h and 48 h. The specific nucleotide levels were shown in Supplementary Table 1 and Table 2. The fold change of the nucleotides were evaluated by comparison of their concentrations in cells treated with RDV and in the parallel controlled RDV-free cells at the same time points. Significant differences in the metabolite profiles of cells with or without RDV were observed. In general, RDV increased the abundance of the majority of RN and dRN species after 24 h incubation, including a greater than 2-fold increase in AMP, GTP, dAMP, dGDP, dGTP, dCTP and TMP levels, then decreased to the normal levels at 48 h (Figure 2 C-F). A rational interpretation was that RDV significantly inhibited the synthesis of nascent RNA and DNA, and arrested the cell cycle in S phase, inevitably resulting in the accumulation of (deoxy)nucleoside triphosphates and subsequently the increase of their respective di- and monophosphates [38]. However, it was notable that most of the pyrimidine ribonucleotides remained unchanged or even declined, among which the significant decrease of CTP was in stark contrast to the 3-fold greater increment of CMP after incubation for 24 h (Figure 2 D). CTP is synthesized from UTP by CTP synthase, which is the rate-limiting step of *de novo* CTP biosynthesis and probably a practical target just as in the treatment of leukemia [39] and parasitic infections [40-42]. In this study, the ratio of CTP/UTP was calculated and shown a significant decrease after 24 incubation (Figure 3 D), implying the inhibition effect of RDV on CTP synthase. Besides of the *de novo* pathway, the salvage pathway plays an important role in cellular nucleotides metabolism as well.

Preprints (www.preprints.org) | NOT PEER-REVIEWED | Posted: 11 December 2020 doi:10.20944/preprints202012.0289.v1

The relative low level of CTP might allosterically activate the recycle of free bases and nucleosides to promote the production of CMP, resulting in the abnormal elevation of CMP (Figure 4).

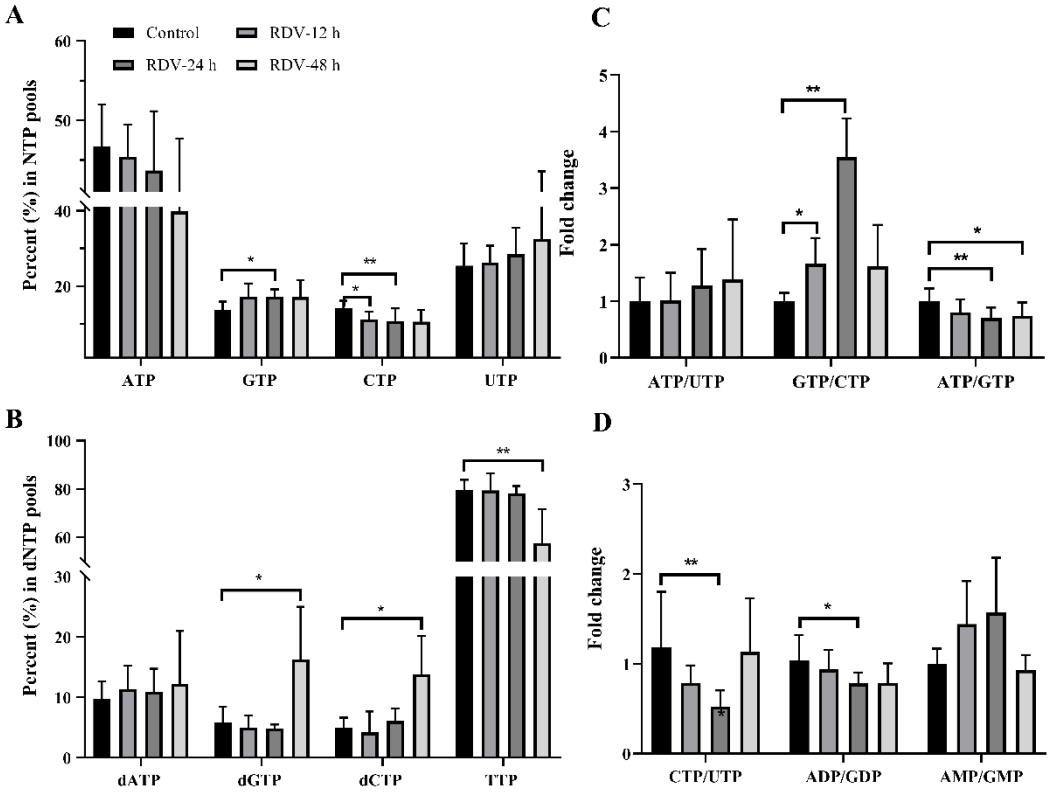

Figure 3. RDV exposure (10 μM) perturbed the balance of (A) NTPs and (B) dNTPs, and altered the relative ratios of specific nucleotides (C and D).

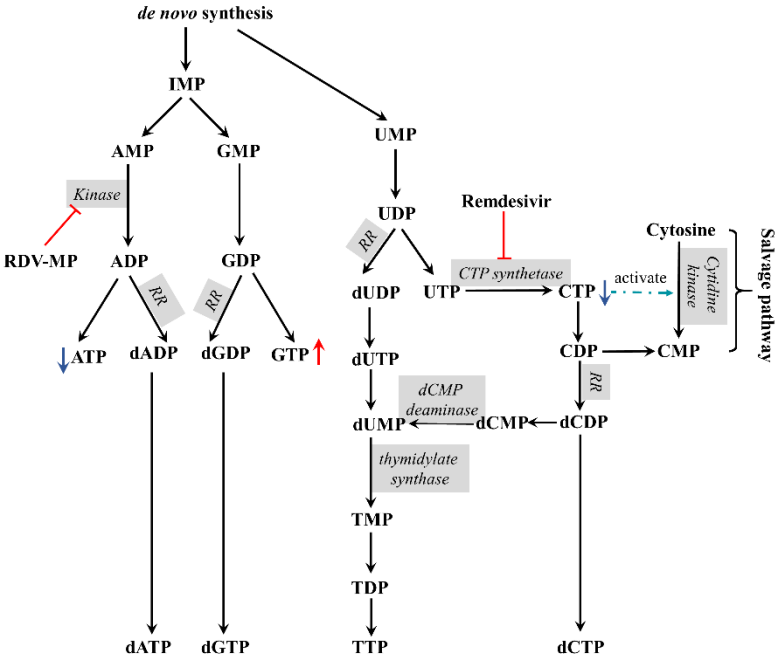

Figure 4. Effect of remdesivir on de novo and salvage pathways of nucleotides synthesis.

The alterations in nucleotide pools were also evaluated through comparing the percent of each NTP in the whole nucleotide pools. It showed that RDV exposure (10 μM) stimulates an increase in GTP and a decrease in CTP (Figure 3 A). Consequently, a significant increment of GTP/CTP was observed (Figure 3 C), indicating the huge disequilibrium in RN pools. Although there were no

Preprints (www.preprints.org) | NOT PEER-REVIEWED | Posted: 11 December 2020 doi:10.20944/preprints202012.0289.v1

statistically significant differences, the level of ATP reduced and UTP increased slightly (Figure 3A), resulting in the elevated ratio of ATP/UTP (Figure 3 C). From the aspect of drug disposition, RDV was hydrolyzed to its corresponding nucleoside monophosphate (RDV-MP) in cell, and furtherly metabolized to RDV-TP. Due to the structural similarity of RDV-MP to AMP, the further phosphorylation of RDV-MP was achieved through the competitive inhibition of adenylate kinase, which inevitably resulted in the accumulation of AMP and the decrease of ADP and ATP. Meanwhile, the accumulation of AMP might inhibited the activity of adenylosuccinate synthase and the whole purine biosynthesis pathway in a negative feedback mode, which would simultaneously decrease the production of GMP, and ultimately GDP and GTP[43]. This speculation was proved by the relative high levels of the AMP/GMP ratio and the reduced ATP/GTP and ADP/GDP ratios at 24 h and 48 h (Figure 3 C and D). The relative percent of dNTPs pools were shown in Figure 3 B. The change of dNTPs percent were just contrary to that of NTPs, and there was obvious hysteresis, which was probably because of the allosteric regulation of NTPs to riboreductase. In summary, RDV exerted the antiviral activity partly via aggravating the imbalance of nucleotide pools, especially through reducing CTP.

2.5. RDV upregulated the riboreductase R2 expression

The remarkably evaluated dNTP pools in cell are probably related with the dNTP synthesis enzymes, especially the ribonucleotide reductase (RR) that catalyzes the formation of deoxyribonucleotides from ribonucleotides [44, 45]. Mammalian RR is comprised of three subunits including RRM1, RRM2 and p53R2, which are expressed in a cell cycle-dependent manner [46]. In cycling cells, the RRM1 protein is metabolically stable throughout the cell cycle whereas the expression and degradation of RRM2 protein limit the S-phase-dependent activity of RR complex, leading to the high cellular dNTPs pools at S phase and low dNTPs pools outside S phase [47]. To further investigated whether the growth inhibitory activity of RDV resulted from the induction of RR, we determined the expression of RRM1, RRM2 and p53R2 by using western blot assay. From the results (Figure 1 C), there' no obvious difference of RRM1 level after the BEAS-2B cells incubated with RDV for 12, 24 and 48 h. However, the expression of RRM2 was significantly increased after 24 h exposure to RDV at 10 μM ($P < 0.05$), which caused by the S phase arrest. At the same time, the p53R2 level presented distinct down-regulated tendency ($P < 0.05$). In addition, there were also no changes in the levels of RRM2 and p53R2 after 48 h incubation with RDV. Taken together, it suggested that RDV inhibited the proliferation of BEAS-2B cells through the impact on RR expression.

3. Discussion

Although authorized for COVID-19 treatment, RDV still cannot meet the clinical needs due to the unsatisfied therapeutic outcome and high mortality [11]. It is therefore urgent to develop new treatment modalities with high efficacy, among which co-administration is a practical strategy. For this purpose, we investigated and found that RDV arrested BEAS-2B cells in the S phase, remarkably inhibited the biosynthesis of nascent RNA and DNA, perturbed RNs and dRNs pool size, and upregulated the expression of riboreductase. Further, based on the action mechanism of RDV, we tried to develop several substances to enhance RDV's antiviral efficacy via a combined strategy. As shown in this study, the RDV-induced decrease of CTP level probably represented a metabolic target for the treatment of COVID-19. The main source of CTP is from the conversion of UTP to CTP by CTP synthase in pyrimidine biosynthesis. Based on the biological property of CTP synthase, co-administration of remdesivir with cyclopentenyl cytosine, an analogue of CTP [48], would be an effective means of sensitizing human bronchial epithelium cells against virus infection. Another helpful strategy might be combination treatment with remdesivir and leflunomide, a clinically approved inhibitor of the *de novo* pyrimidine synthesis pathway, to reduce the CTP production as realized in the reversion of drug resistance of triple-negative breast cancer (TNBC) [32].

4. Materials and Methods

Preprints (www.preprints.org) | NOT PEER-REVIEWED | Posted: 11 December 2020 doi:10.20944/preprints202012.0289.v1

4.1 Reagents and chemicals

3-(4,5-dimethylthiazol-2-yl)-2,5-diphenyltetrazolium bromide (MTT), dimethyl sulfoxide (DMSO), paraformaldehyde (PFA), propidium iodide (PI), 0.05 % RNase A were provided by Sigma-Aldrich Inc. (St. Louis, MO, USA). RDV was purchased from Manhey Chemical Limited (Hong Kong, China). For our experiments, the stock solution of RDV was prepared in DMSO, stored at -20 ℃ and serially diluted in Dulbecco's Modified Eagle's Medium (DMEM) until needed. The final DMSO concentration did not exceed 0.1% throughout this study. 5-ethynyl uridine (EU) and 5-ethynyl-2'-deoxyuridine (EdU) were supplied by Tokyo Chemical Industry Co., Ltd. (Shanghai, China). 4', 6-Diamidino-2-phenylindole (DAPI) and Alexa Fluor™ 594 were purchased from Invitrogen Co. (Carlsbad, CA, USA). Glycine, Tris, $CuSO_4$, ascorbic acid, EDTA, Triton™ X-100 and TWEEN®20 were also obtained from Sigma-Aldrich Inc. RIPA buffer (Cell Signaling Technologies Inc. Beverly, MA, USA), Bradford reagent (Bio-Rad Laboratory, Hercules, CA, USA), nitrocellulose membrane (Merck Millipore, USA) and the enhanced chemiluminescence reagents (Invitrogen, Paisley, Scotland, UK) were also used in this study. For cell culture, DMEM, fetal bovine serum (FBS), penicillin-streptomycin solution, phosphate Buffer Saline (PBS) and 0.25 % Trypsin-EDTA solution were obtained from GIBCO (Grand Island, NY, USA).

The stable isotope labeled adenosine-$^{13}C_{10}$,$^{15}N_5$-triphosphate (ATP-$^{13}C_{10}$,$^{15}N_5$) and adenosine-$^{13}C_{10}$,$^{15}N_5$-monophosphate (AMP-$^{13}C_{10}$,$^{15}N_5$), other nucleotide standards and ammonium acetate (NH_4OAc) were purchased from Sigma-Aldrich Inc. (St. Louis, MO, USA). TMSD and tetrafluoroboric acid (HBF4) were obtained from Alfa Aesar Co. (Ward Hill, MA, USA). The methanol (LC-MS grade) and acetonitrile used for the LC-MS/MS analysis were bought from Anaqua Chemical Supply (Houston, TX, USA). Formic acid was bought from Fisher Scientific Co. (Fair Lawn, NJ, USA) and diethyl ether was obtained from Tedia Co. (Fairfield, OH, USA) while acetic acid (AcOH) and 30% ammonium hydroxide aqueous solution (NH_4OH) were purchased from J. T. Baker Chemical Co. (Phillipsburg, NJ, USA). The solid phase extraction (SPE) cartridges (WAX, 3 cm^3; 30 mg, 60 μm) was bought from Waters Co. (Milford, MA, USA) while the chromatographic column Sepax GP-C_{18} (2.1 × 150 mm2, 1.8 μm) from Sepax Technologies (Newark, DE, USA) was also used. Ultrapure water was obtained on the basis of a Milli-Q Gradient water system (Millipore, Bedford, MA, USA).

4.2 Cell culture and colorimetric MTT assay

BEAS-2B cells were purchased from the ATCC (Manassas, VA, United States). They were cultured in DMEM supplemented with 10% FBS, 100 U/mL penicillin-streptomycin in a humidified incubator at 37 °C and 5% CO_2. Cell viability was determined by a modified colorimetric MTT assay [34]. Briefly, the logarithmic BEAS-2B cells at 6.0 × 10^4 cells/mL were seeded in a 96-well plate at 100 μL/well for 24 h at 37 °C, then treated with RDV at different concentrations (0-100 μM) for 24, 48 and 72 h, respectively. After the appropriate incubation time, 10 μL MTT solution (5 mg/mL) was added for another 4 h incubation, and 100 μL DMSO was added to dissolve formazan crystals for the further measurement at 570 nm using a microplate ultraviolet-visible spectrophotometer. Cell viability was calculated as follows: cell viability (%) = (absorbance of the test group/absorbance of the control group) × 100. The IC_{50} value was taken as the concentration that caused 50% inhibition of cell viability and was calculated by GraphPad Prism. (Graph-Pad Software, Inc., La Jolla, CA, USA).

4.3 EU and EdU detection using click chemistry

In order to label and visualize specifically newly synthesized DNA and RNA, the click chemistry method was used. The experiments were conducted based on previous publications with slight modification [35, 36]. In short, BEAS-2B cells were grown in 6-well plate at 2.0 × 10^5 cells/well for 24 h and then incubated for 14 h with 1.0 mM EU or 10 μM EdU in the presence or absence of 10 μM RDV. After the labeling, cells were washed with PBS and fixed with 4% PFA for 30 min. The fixed cells were neutralized with 2 mg/mL glycine, rinsed with PBS and stained for 30 min at room temperature with a click reaction buffer including 100 mM Tris, 1 mM CuSO4, 10 μM Alexa594-azide and 100 mM ascorbic acid. After staining, cells were washed several times by using PBS with 0.5 mM

Preprints (www.preprints.org) | NOT PEER-REVIEWED | Posted: 11 December 2020 doi:10.20944/preprints202012.0289.v1

EDTA, 1% TWEEN®20 and 0.1% Triton™ X-100, and then stained with 0.5 μg/mL DAPI for 30 min. Finally, the cells were imaged by IncuCyte ZOOM Live-Cell Analysis Platform.

4.4 Cell cycle analysis

BEAS-2B cells were seeded in 6-plate at 2.0 × 10^5 cells/well, cultured for 24 h and then treated with/without RDV for 12, 24 and 48 h, respectively. Then, the cells were harvested, re-suspended in ice-cold PBS and fixed with 70 % ethanol at -20 ℃ overnight. Subsequently, the fixed cells were washed again using ice-cold PBS and incubated with 500 μL PI containing 0.05 % RNase A for 30 min at room temperature in the dark circumstances. Finally, cell cycle distribution profile after the staining treatment was accessed by flow cytometry. The percentages of cells in G0/G1, S and G2/M phases were analyzed by using MODFIT software (Verity Sofware House, USA).

4.5 Western blot assay

BEAS-2B cells were treated with RDV at the indicated concentration for 12, 24 and 48 h, respectively. Then the cells were washed with cold PBS twice and lysed with RIPA buffer on ice. The lysates were centrifuged at 12000 g for 30 min at 4 ℃ in order to acquire the protein samples. The concentration of cellular total protein was measured by using the Bradford reagent at 595 nm according to the manufacturer's instructions. 30 μg protein samples were loaded on 10% SDS-PAGE gel and transferred to onto nitrocellulose membranes. The membranes were blocked with 5% skim milk for 1.5 h, followed by the incubation of primary antibodies diluted in Tris-buffered saline with Tween® 20 (TBST) buffer. (1:1000 for β-tubulin, RRM1, RRM2 and P53R2, Cell Signaling Technologies, Danvers, MA) overnight at 4 ℃. After that, the membranes were washed with TBST and incubated with secondary horseradish peroxidase-conjugated antibody anti-rabbit IgG (Cell Signaling Technologies, Inc. Danvers, MA, USA) for 1 h at room temperature. The immunoreactive protein bands were finally detected with an Amersham Imager 600 Western blotting system. Densitometry analysis of protein band was performed by Quantity One software (Version 4.6.2, Bio-Rad, USA).

4.6 Sample preparation and LC-MS/MS analysis

BEAS-2B cells were plated in 10 cm petri dishes with the density of 2.0 × 10^6 cells/dish, cultured with medium for 24 h and then treated with RDV for 12, 24 and 48 h, respectively. After that, the cells were re-suspended with ice-cold PBS. The number of cells was counted before centrifugation at 1200 rpm for 5 min, and the cell pellet was washed with 1.0 mL ice-cold PBS again and spun down at 1200 rpm for 5 min. Subsequently cell pellets were treated with 150 μL 80% methanol containing 4 μM AMP-$^{13}C_{10}$,$^{15}N_5$ and 2 μM ATP-$^{13}C_{10}$,$^{15}N_5$ as an internal standards (IS). The following sample preparation and the determination of endogenous RNs and dRNs were performed based on the method previously described [33]. The concentrations of cellular nucleotides were finally calculated according to dividing the absolute amount of each RN and dRN in each sample by the corresponding cell number.

4.7 Statistics analysis

Data analyses were performed using GraphPad Prism software and the values were expressed as mean ± standard deviation (SD) from three independent replicate experiments. The statistical significance of the comparison between control and treated groups was determined by Student's t-test or one-way ANOVA, which is indicated as *$P < 0.05$ and **$P < 0.01$.

Supplementary Materials: Supplementary materials can be found at www.mdpi.com/xxx/s1.

Author Contributions: Conceptualization, W.Z, Y.L. and H.Z.; methodology, W.Z, Y.L. and H.Z.; software, W.L; validation, Y.L., H.Z.; formal analysis, C.W.; investigation, W.Z, H.Z. L.B.; resources, W.Z, Z.J. and V.K.W.W.; data curation, Y.L., H.Z.; writing—original draft preparation, H.Z. and Y.L.; writing—review and editing,

Preprints (www.preprints.org) | NOT PEER-REVIEWED | Posted: 11 December 2020 doi:10.20944/preprints202012.0289.v1

C.W.K.L., W.Z., and V.K.W.W.; visualization, C.W.; project administration, W.Z. and Z.J.; funding acquisition, W.Z.. All authors have read and agreed to the published version of the manuscript.

Funding: This research was funded by the Science and Technology Development Fund, Macau SAR (File no. 0033/2020/A and 0023/2019/AKP).

Acknowledgments: The authors also thank the Department of Science and Technology of Guangdong Province for the support of Guangdong-Hong Kong-Macao Joint Laboratory of Respiratory Infectious Disease.

Conflicts of Interest: The authors declare no conflict of interest.

Abbreviations

RDV	Remdesivir
COVID-19	2019 novel coronavirus
RNA	Ribonucleic acid
DNA	Deoxyribonucleic acid
RdRps	RNA-dependent RNA polymerases
RDV-MP	Remdesivir nucleoside monophosphate
RDV-DP	Remdesivir nucleoside diphosphate
RDV-TP	Remdesivir nucleoside triphosphate
RNs	Ribonucleotides
dRNs	Deoxyribonucleotides
NTPs	Ribonucleoside triphosphates
dNTPs	Deoxyribonucleoside triphosphates
AMP	Adenosine monophosphate
GMP	Guanosine monophosphate
IMP	Inosine monophosphate
UMP	Uridine monophosphate
CMP	Cytidine monophosphate
ADP	Adenosine diphosphate
GDP	Guanosine diphosphate
UDP	Uridine diphosphate
CDP	Cytidine diphosphate
ATP	Adenosine triphosphate
GTP	Guanosine triphosphate
CTP	Cytidine triphosphate
dAMP	Deoxyadenosine monophosphate
dGMP	Deoxyguanosine monophosphate
dUMP	Deoxyuridine monophosphate
TMP	Thymidine monophosphate
dCMP	Deoxycytidine monophosphate
dADP	Deoxyadenosine diphosphate
dGDP	Deoxyguanosine diphosphate;
dUDP	Deoxyuridine diphosphate
TDP	Thymidine diphosphate
dCDP	Deoxycytidine diphosphate
dATP	Deoxyadenosine triphosphate
dGTP	Deoxyguanosine triphosphate
dUTP	Deoxyuridine triphosphate
TTP	Thymidine triphosphate
dCTP	Deoxycytidine triphosphate
HPLC-MS/MS	High-performance liquid chromatography− tandem mass spectrometry

References

1. Warren, T.K.; Jordan, R.; Lo, M.K.; Ray, A.S.; Mackman, R.L.; Soloveva, V.; Siegel, D.; Perron, M.;

Preprints (www.preprints.org) | NOT PEER-REVIEWED | Posted: 11 December 2020 doi:10.20944/preprints202012.0289.v1

Bannister, R.; Hui, H.C.; Larson, N.; Strickley, R.; Wells, J.; Stuthman, K.S.; Van Tongeren, S.A.; Garza, N.L.; Donnelly, G.; Shurtleff, A.C.; Retterer, C.J.; Gharaibeh, D.; Zamani, R.; Kenny, T.; Eaton, B.P.; Grimes, E.; Welch, L.S.; Gomba, L.; Wilhelmsen, C.L.; Nichols, D.K.; Nuss, J.E.; Nagle, E.R.; Kugelman, J.R.; Palacios, G.; Doerffler, E.; Neville, S.; Carra, E.; Clarke, M.O.; Zhang, L.; Lew, W.; Ross, B.; Wang, Q.; Chun, K.; Wolfe, L.; Babusis, D.; Park, Y.; Stray, K.M.; Trancheva, I.; Feng, J.Y.; Barauskas, O.; Xu, Y.; Wong, P.; Braun, M.R.; Flint, M.; McMullan, L.K.; Chen, S.S.; Fearns, R.; Swaminathan, S.; Mayers, D.L.; Spiropoulou, C.F.; Lee, W.A.; Nichol, S.T.; Cihlar, T.; Bavari, S. Therapeutic efficacy of the small molecule GS-5734 against Ebola virus in rhesus monkeys. *Nature* **2016,** *531*, (7594), 381-385, doi: 10.1038/nature17180.

2. Sheahan, T.P.; Sims, A.C.; Graham, R.L.; Menachery, V.D.; Gralinski, L.E.; Case, J.B.; Leist, S.R.; Pyrc, K.; Feng, J.Y.; Trantcheva, I.; Bannister, R.; Park, Y.; Babusis, D.; Clarke, M.O.; Mackman, R.L.; Spahn, J.E.; Palmiotti, C.A.; Siegel, D.; Ray, A.S.; Cihlar, T.; … Baric, R.S.. Broad-spectrum antiviral GS-5734 inhibits both epidemic and zoonotic coronaviruses. *Sci. Transl. Med.* **2017,** *9*, (396), eaal3653, doi: 10.1126/scitranslmed.aal3653.
3. Lo, M.K.; Feldmann, F.; Gary, J.M.; Jordan, R.; Bannister, R.; Cronin, J.; Patel, N.R.; Klena, J.D.; Nichol, S.T.; Cihlar, T.; Zaki, S.R.; Feldmann, H.; Spiropoulou, C.F.; de Wit, E.. Remdesivir (GS-5734) protects African green monkeys from Nipah virus challenge. *Sci. Transl. Med.* **2019,** *11*, (494), eaau9242, doi: 10.1126/scitranslmed.aau9242.
4. Sheahan, T.P.; Sims, A.C.; Leist, S.R.; Schafer, A.; Won, J.; Brown, A.J.; Montgomery, S.A.; Hogg, A.; Babusis, D.; Clarke, M.O.; Spahn, J.E.; Bauer, L.; Sellers, S.; Porter, D.; Feng, J.Y.; Cihlar, T.; Jordan, R.; Denison, M.R.; Baric, R.S. Comparative therapeutic efficacy of remdesivir and combination lopinavir, ritonavir, and interferon beta against MERS-CoV. *Nat. Commun.* **2020,** *11*, (1), 1-14, doi: 10.1038/s41467-019-13940-6.
5. de Wit, E.; Feldmann, F.; Cronin, J.; Jordan, R.; Okumura, A.; Thomas, T.; Scott, D., Cihlar, T.; Feldmann, H.. Prophylactic and therapeutic remdesivir (GS-5734) treatment in the rhesus macaque model of MERS-CoV infection. *PNAS* **2020,** *117*, (12), 6771-6776, doi: 10.1073/pnas.1922083117.
6. Jacobs, M.; Rodger, A.; Bell, D.J.; Bhagani, S.; Cropley, I.; Filipe, A.; Gifford, R.J.; Hopkins, S.; Hughes, J.; Jabeen, F.; Johannessen, I.; Karageorgopoulos, D.; Lackenby, A.; Lester, R.; Liu, R.S.; MacConnachie, A.; Mahungu, T.; Martin, D.; Marshall, N.; Mepham, S.; Orton, R.; Palmarini, M.; Patel, M.; Perry, C.; Peters, S.E.; Porter, D.; Ritchie, D.; Ritchie, N.D.; Seaton, R.A.; Sreenu, V.B.; Templeton, K.; Warren, S.; Wilkie, G.S.; Zambon, M.; Gopal, R.; Thomson, E.C.. Late Ebola virus relapse causing meningoencephalitis: a case report. *The Lancet* **2016,** *388*, (10043), 498-503, doi: 10.1016/S0140-6736(16)30386-5.
7. Dornemann, J.; Burzio, C.; Ronsse, A.; Sprecher, A.; De Clerck, H.; Van Herp, M.; Kolie, M.C.; Yosifiva, V.; Caluwaerts, S.; McElroy, A.K.; Antierens, A. First Newborn Baby to Receive Experimental Therapies Survives Ebola Virus Disease. *J. Infect. Dis.* **2017,** *215*, (2), 171-174, doi: 10.1093/infdis/jiw493.
8. Mulangu, S.; Dodd, L.E.; Davey, R.T. Jr.; Tshiani Mbaya, O.; Proschan, M.; Mukadi, D.; Lusakibanza Manzo, M.; Nzolo, D.; Tshomba Oloma, A.; Ibanda, A.; Ali, R.; Coulibaly, S.; Levine, A.C.; Grais, R.; Diaz, J.; Lane, H.C.; Muyembe-Tamfum, J.J.; PALM Writing Group; Sivahera, B.; Camara, M.; Kojan, R.; Walker, R.; Dighero-Kemp, B.; Cao H.; Mukumbayi, P.; Mbala-Kingebeni, P.; Ahuka, S.; Albert, S.; Bonnett, T.; Crozier, I.; Duvenhage, M.; Proffitt, C.; Teitelbaum, M.; Moench, T.; Aboulhab, J.; Barrett, K.; Cahill, K.; Cone, K.; Eckes, R.; Hensley, L.; Herpin, B.; Higgs, E.; Ledgerwood, J.; Pierson, J.; Smolskis, M.; Sow, Y.; Tierney, J.; Sivapalasingam, S.; Holman, W.; Gettinger, N.; Vallée, D.; Nordwall,

Preprints (www.preprints.org) | NOT PEER-REVIEWED | Posted: 11 December 2020 doi:10.20944/preprints202012.0289.v1

J.; PALM Consortium Study Team. A Randomized, Controlled Trial of Ebola Virus Disease Therapeutics. *N. Engl. J. Med.* **2019,** *381*, (24), 2293-2303, doi: 10.1056/NEJMoa1910993.

9. Holshue, M.L.; DeBolt, C.; Lindquist, S.; Lofy, K.H.; Wiesman, J.; Bruce, H.; Spitters, C.; Ericson, K.; Wilkerson, S.; Tural, A.; Diaz, G.; Cohn, A.; Fox, L.; Patel, A.; Gerber, S. I.; Kim, L.; Tong, S.; Lu, X.; Lindstrom, S.; Pallansch, M.A.; Weldon, W.C.; Biggs, H.M.; Uyeki, T.M.; Pillai, S.K.; Washington State 2019-nCoV Case Investigation Team. First Case of 2019 Novel Coronavirus in the United States. *N. Engl. J. Med.* **2020,** *382*, (10), 929-936, doi: 10.1056/NEJMoa2001191.
10. Wang, M., Cao, R., Zhang, L., Yang, X., Liu, J., Xu, M., Shi, Z., Hu, Z., Zhong, W., Xiao, G.. Remdesivir and chloroquine effectively inhibit the recently emerged novel coronavirus (2019-nCoV) in vitro. *Cell Res.* **2020,** *30*, (3), 269-271, doi: 10.1038/s41422-020-0282-0.
11. Beigel, J.H.; Tomashek, K.M.; Dodd, L.E.; Mehta, A.K.; Zingman, B.S.; Kalil, A.C.; Hohmann, E.; Chu, H.Y.; Luetkemeyer, A.; Kline, S.; Lopez de Castilla, D.; Finberg, R.W.; Dierberg, K.; Tapson, V.; Hsieh, L.; Patterson, T.F.; Paredes, R.; Sweeney, D.A.; Short, W.R.; Touloumi, G.; Lye, D.C.; Ohmagari, N.; Oh, M.D.; Ruiz-Palacios, G.M.; Benfield, T.; Fatkenheuer, G.; Kortepeter, M.G.; Atmar, R.L.; Creech, C.B.; Lundgren, J.; Babiker, A.G.; Pett, S.; Neaton, J.D.; Burgess, T.H.; Bonnett, T.; Green, M.; Makowski, M.; Osinusi, A.; Nayak, S.; Lane, H.C.; Members, A.-S.G. Remdesivir for the Treatment of Covid-19 - Preliminary Report. *N. Engl. J. Med.* **2020**, doi: 10.1056/NEJMoa2007764.
12. US Food and Drug Administration. Administration, U. F. D. Authorization for emergency use of remdesivir for the treatment of COVID-19 (letter). https://www.fda.gov/media/137564/download. May 1, 2020.
13. Tchesnokov, E.P.; Feng, J.Y.; Porter, D.P.; Gotte, M. Mechanism of Inhibition of Ebola Virus RNA-Dependent RNA Polymerase by Remdesivir. *Viruses* **2019,** *11*, (4), 326-341, doi: 10.3390/v11040326.
14. Ju, J.; Li, X.; Kumar, S.; Jockusch, S.; Chien, M.; Tao, C.; Morozova, I.; Kalachikov, S.; Kirchdoerfer, R.N.; Russo, J.J. Nucleotide Analogues as Inhibitors of SARS-CoV Polymerase. *bioRxiv* **2020**, March 14, doi: 10.1101/2020.03.12.989186.
15. Luengo, A.; Gui, D.Y.; Vander Heiden, M.G. Targeting Metabolism for Cancer Therapy. *Cell Chem. Biol.* **2017,** *24*, (9), 1161-1180, doi: 10.1016/j.chembiol.2017.08.028.
16. Ip, W.E.; Hoshi, N.; Shouval, D.S.; Snapper, S.; Medzhitov, R.. Anti-inflammatory effect of IL-10 mediated by metabolic reprogramming of macrophages. *Science* **2017,** *356*, (6337), 513-519, doi: 10.1126/science.aal3535.
17. Lee, W.A.; He, G.X.; Eisenberg, E.; Cihlar, T.; Swaminathan, S.; Mulato, A.; Cundy, K.C. Selective intracellular activation of a novel prodrug of the human immunodeficiency virus reverse transcriptase inhibitor tenofovir leads to preferential distribution and accumulation in lymphatic tissue. *Antimicrob. Agents Chemother.* **2005,** *49*, (5), 1898-906, doi: 10.1128/AAC.49.5.1898-1906.2005.
18. Ray, A.S.; Fordyce, M.W.; Hitchcock, M.J. Tenofovir alafenamide: A novel prodrug of tenofovir for the treatment of Human Immunodeficiency Virus. *Antiviral. Res.* **2016,** *125*, 63-70, doi: 10.1016/j.antiviral.2015.11.009.
19. Siegel, D.; Hui, H.C.; Doerffler, E.; Clarke, M.O.; Chun, K.; Zhang, L.; Neville, S.; Carra, E.; Lew, W.; Ross, B.; Wang, Q.; Wolfe, L.; Jordan, R.; Soloveva, V.; Knox, J.; Perry, J.; Perron, M.; Stray, K.M.; Barauskas, O.; Feng, J.Y.; Xu, Y.; Lee, G.; Rheingold, A.L.; Ray, A.S.; Bannister, R.; Strickley, R.; Swaminathan, S.; Lee, W.A.; Bavari, S.; Cihlar, T.; Lo, M.K.; Warren, T.K.; Mackman, R.L. Discovery and Synthesis of a Phosphoramidate Prodrug of a Pyrrolo[2,1-f][triazin-4-amino] Adenine C-Nucleoside (GS-5734) for the Treatment of Ebola and Emerging Viruses. *J. Med. Chem.* **2017,** *60*, (5), 1648-1661,

Preprints (www.preprints.org) | NOT PEER-REVIEWED | Posted: 11 December 2020 doi:10.20944/preprints202012.0289.v1

doi: 10.1021/acs.jmedchem.6b01594.

20. Cho, A.; Saunders, O.L.; Butler, T.; Zhang, L.; Xu, J.; Vela, J.E.; Feng, J.Y.; Ray, A.S.; Kim, C.U. Synthesis and antiviral activity of a series of 1'-substituted 4-aza-7,9-dideazaadenosine C-nucleosides. *Bioorg. Med. Chem. Lett.* **2012,** *22*, (8), 2705-7, doi: 10.1016/j.bmcl.2012.02.105.
21. Williamson, B.N.; Feldmann, F.; Schwarz, B.; Meade-White, K.; Porter, D.P.; Schulz, J.; van Doremalen, N.; Leighton, I.; Yinda, C.K.; Perez-Perez, L.; Okumura, A.; Lovaglio, J.; Hanley, P.W.; Saturday, G.; Bosio, C.M.; Anzick, S.; Barbian, K.; Cihlar, T.; Martens, C.; Scott, D.P.; Munster, V.J.; de Wit, E.. Clinical benefit of remdesivir in rhesus macaques infected with SARS-CoV-2. *Nature* **2020**, 1-6, doi: 10.1038/s41586-020-2423-5.
22. Yan, V.C.; Muller, F.L.. Advantages of the Parent Nucleoside GS-441524 over Remdesivir for Covid-19 Treatment. *ACS. Med. Chem. Lett.* **2020,** *11*, (7), 1361-1366, doi: 10.1021/acsmedchemlett.0c00316.
23. Boccardo G.; Accotto, G.P.. RNA-Dependent RNA Polymerase Activity in Two Morphologically Different White Clover Cryptic Viruses. *Virology* **1988,** *163*, (2), 413-419, doi: 10.1016/0042-6822(88)90282-6.
24. Fahima T., Kazmierczak P., Hansen D.R., Pfeiffer P., Van Alfen N.K.. Membrane-Associated Replication of an Unencapsidated Double-Strand RNA of the Fungus, Cryphonectria parasitica. *Virology* **1993,** *195*, (1), 81-89, doi: 10.1006/viro.1993.1348.
25. Stridh, S.. Determination of Ribonneleoside Triphosphate Pools in Influenza A Virus-Infected MDCK Cells. *Arch. Virol* **1983,** *77*, (2-4), 223-229, doi: 10.1007/BF01309269.
26. Balzarini J., Karlsson A., Wang L., Bohman C., Horská K., Votruba I., Fridland A., Van Aerschot A., Herdewijn P., De Clercq E.. Eicar (5-ethynyl-1-beta-D-ribofuranosylimidazole-4-carboxamide). A novel potent inhibitor of inosinate dehydrogenase activity and guanylate biosynthesis. *The Journal of Biological Chemistry* **1993,** *268*, (33), 24591-24598.
27. De Clercq, E.. New Nucleoside Analogues for the Treatment of Hemorrhagic Fever Virus Infections. *Chem Asian J* **2019,** *14*, (22), 3962-3968, doi: 10.1002/asia.201900841.
28. Bistulfi, G.; Diegelman, P.; Foster, B.A.; Kramer, D.L.; Porter, C.W.; Smiraglia, D.J. Polyamine biosynthesis impacts cellular folate requirements necessary to maintain S-adenosylmethionine and nucleotide pools. *FASEB J.* **2009,** *23*, (9), 2888-97, doi: 10.1096/fj.09-130708.
29. Jang, K.J.; Jeong, S.; Kang, D.Y.; Sp, N.; Yang, Y.M.; Kim, D.E. A high ATP concentration enhances the cooperative translocation of the SARS coronavirus helicase nsP13 in the unwinding of duplex RNA. *Sci. Rep.* **2020,** *10*, (1), 4481-4493, doi: 10.1038/s41598-020-61432-1.
30. Vander Heiden M.G.; DeBerardinis, R.J.. Understanding the Intersections between Metabolism and Cancer Biology. *Cell* **2017,** *168*, (4), 657-669, doi: 10.1016/j.cell.2016.12.039.
31. Mathews, C.K. Deoxyribonucleotides as genetic and metabolic regulators. *FASEB J.* **2014,** *28*, (9), 3832-40, doi: 10.1096/fj.14-251249.
32. Brown, K.K.; Spinelli, J.B.; Asara, J.M.; Toker, A. Adaptive Reprogramming of De Novo Pyrimidine Synthesis Is a Metabolic Vulnerability in Triple-Negative Breast Cancer. *Cancer Discov.* **2017,** *7*, (4), 391-399, doi: 10.1158/2159-8290.CD-16-0611.
33. Li, Z.; Zhang, H.X.; Li, Y.; Lam, C.W.K.; Wang, C.Y.; Zhang, W.J.; Wong, V.K.W.; Pang, S.S.; Yao, M.C.; Zhang, W.. Method for Quantification of Ribonucleotides and Deoxyribonucleotides in Human Cells Using (Trimethylsilyl)diazomethane Derivatization Followed by Liquid Chromatography-Tandem Mass Spectrometry. *Anal. Chem.* **2019,** *91*, (1), 1019-1026, doi: 10.1021/acs.analchem.8b04281.
34. van Meerloo, J.; Kaspers, G.J.; Cloos, J. Cell sensitivity assays: the MTT assay. *Methods Mol. Biol.* **2011,** *731*, 237-45, doi: 10.1007/978-1-61779-080-5_20.

Preprints (www.preprints.org) | NOT PEER-REVIEWED | Posted: 11 December 2020 doi:10.20944/preprints202012.0289.v1

35. Jao, C.Y.; Salic, A.. Exploring RNA transcription and turnover in vivo by using click chemistry. *Proc. Natl. Acad. Sci. USA.* **2008,** *105*, (41), 15779-84, doi: 10.1073/pnas.0808480105.
36. Akbalik, G.; Langebeck-Jensen, K.; Tushev, G.; Sambandan, S.; Rinne, J.; Epstein, I.; Cajigas, I.; Vlatkovic, I.; Schuman, E.M. Visualization of newly synthesized neuronal RNA in vitro and in vivo using click-chemistry. *RNA Biol.* **2017,** *14*, (1), 20-28, doi: 10.1080/15476286.2016.1251541.
37. Qu, D.; Wang, G.; Wang, Z.; Zhou, L.; Chi, W.; Cong, S.; Ren, X.; Liang, P.; Zhang, B. 5-Ethynyl-2'-deoxycytidine as a new agent for DNA labeling: detection of proliferating cells. *Anal. Biochem.* **2011,** *417*, (1), 112-121, doi: 10.1016/j.ab.2011.05.037.
38. Du, L.; Yang, F.; Fang, H.; Sun, H.; Chen, Y.; Xu, Y.; Li, H.; Zheng, L.; Zhou, B.S. AICAr suppresses cell proliferation by inducing NTP and dNTP pool imbalances in acute lymphoblastic leukemia cells. *FASEB J.* **2019,** *33*, (3), 4525-4537, doi: 10.1096/fj.201801559RR.
39. Verschuur, A.; Van Gennip, A.; Muller, E.; Voute, P.; Van Kuilenburg, A.. Increased Activity of Cytidinetriphosphate Synthetase in Pediatric Acute Lymphoblastic Leukemia. In *Purine and pyrimidine metabolism in man IX*, Springer: 1998; pp 667-671.
40. Fijolek, A.; Hofer, A.; Thelander, L. Expression, purification, characterization, and in vivo targeting of trypanosome CTP synthetase for treatment of African sleeping sickness. *J. Biol. Chem.* **2007,** *282*, (16), 11858-11865, doi: 10.1074/jbc.M611580200.
41. Hofer, A.; Steverding, D.; Chabes, A.; Brun, R.; Thelander, L.. Trypanosoma brucei CTP synthetase: a target for the treatment of African sleeping sickness. *Proceedings of the National Academy of Sciences* **2001,** *98*, (11), 6412-6416, doi: 10.1073/pnas.111139498.
42. Tamborini, L.; Pinto, A.; Smith, T.K.; Major, L.L.; Iannuzzi, M.C.; Cosconati, S.; Marinelli, L.; Novellino, E.; Presti, L.L.; Wong, P.E.. Synthesis and biological evaluation of CTP synthetase inhibitors as potential agents for the treatment of African trypanosomiasis. *ChemMedChem* **2012,** *7*, (9), 1623-1634, doi: 10.1002/cmdc.201200304.
43. Nelson, D.L.; Lehninger A.L.; Cox, M.M.. *Lehninger principles of biochemistry (4th ed.)*. 2008. 862 p.
44. Liu, B.; Grosshans, J.. The role of dNTP metabolites in control of the embryonic cell cycle. *Cell Cycle* **2019,** *18*, (21), 2817-2827, doi: 10.1080/15384101.2019.1665948.
45. Mathews, C.K. DNA precursor metabolism and genomic stability. *FASEB J.* **2006,** *20*, (9), 1300-14, doi: 10.1096/fj.06-5730rev.
46. Yousefi, B.; Samadi, N.; Ahmadi, Y.. Akt and p53R2, partners that dictate the progression and invasiveness of cancer. *DNA Repair (Amst)* **2014,** *22*, 24-9, doi: 10.1016/j.dnarep.2014.07.001.
47. Engström Y.; Eriksson S.; Jildevik I.; Skog S.; Thelander, L.; Tribukait, B.. Cell cycle-dependent expression of mammalian ribonucleotide reductase. Differential regulation of the two subunits. *J. Biol. Chem.* **1985,** *260*, 9114-9116.
48. Kang, G.J.; Cooney, D.A.; Moyer, J.D.; Kelley, J.A.; Kim, H.Y.; Marquez, V.E.; Johns, D.G.. Cyclopentenylcytosine triphosphate. Formation and inhibition of CTP synthetase. *J. Biol. Chem.* **1989,** *264*, (2), 713-718.